25th ABCM International Congress of Mechanical Engineering
October 20-25, 2019, Uberlândia, MG, Brazil

COB-2019- 0537
APPLICATION OF THE FINITE DIFFERENCES METHOD FOR NUMERICAL SIMULATION OF THE COUETTE FLOW

Giovanna Bruna dos Santos
Instituto Federal de Educação, Ciência e Tecnologia de Alagoas
Avenida Alagoas - até 109/110, São Cristóvão, Palmeira dos Índios, AL
giovanna-brunna@hotmail.com

Mahelvson Bazilio Chaves
Instituto Federal de Educação, Ciência e Tecnologia de Alagoas
Avenida Alagoas - até 109/110, São Cristóvão, Palmeira dos Índios, AL
mahelvson@gmail.com

Abstract. *Due to the complexity of the Navier-Stokes equations, since they are presented as a second order system and a nonlinear partial differential equations that describes the behavior of the fluid movement, they have, mainly, a few analytical solutions restricted to some particular cases. With the development of Computational Fluid Dynamics (CFD), through the application of numerical methods, it has been possible to solve them for more complex cases, providing a better comprehension of fluid flow process. The goal of this work is to demonstrate the application of Crank-Nicolson semi-implicit scheme for finite differences method to solve Couette incompressible flow with the pressure gradient in order to find the best time intervals and spatial discretization that provides accurate results with low computational cost. The best result was obtained for small spatial discretization and time intervals according to the accuracy that was defined as satisfactory.*

Keywords: *Couette flow, Finite Difference Method, Crank-Nicolson Semi-implicit Method, Computational Fluid Dynamics.*

1. INTRODUCTION

Fluid Mechanics obtained more significant contributions from the 19th century with the works of Navier (1822), Poisson (1829) and Stokes (1845) in the formulation of the Navier-Stokes equations which mathematically describe the behavior of Newtonian fluids and are result of the continuity (Eq. (1)) and the momentum equations (Eq. (2), (3), (4)), (Fortuna, 2000). They can be written in general form for three-dimensional and incompressible flow in cartesian coordinates:

$$\frac{\partial u}{\partial x}+\frac{\partial v}{\partial y}+\frac{\partial w}{\partial z}=0 \tag{1}$$

$$\rho\left(\frac{\partial u}{\partial t}+u\frac{\partial u}{\partial x}+v\frac{\partial u}{\partial y}+z\frac{\partial u}{\partial z}\right)=\rho g_x-\frac{\partial p}{\partial x}+\mu\left(\frac{\partial^2 u}{\partial x^2}+\frac{\partial^2 u}{\partial y^2}+\frac{\partial^2 u}{\partial z^2}\right) \tag{2}$$

$$\rho\left(\frac{\partial v}{\partial t}+u\frac{\partial v}{\partial x}+v\frac{\partial v}{\partial y}+z\frac{\partial v}{\partial z}\right)=\rho g_y-\frac{\partial p}{\partial y}+\mu\left(\frac{\partial^2 v}{\partial x^2}+\frac{\partial^2 v}{\partial y^2}+\frac{\partial^2 v}{\partial z^2}\right) \tag{3}$$

$$\rho\left(\frac{\partial w}{\partial t}+u\frac{\partial w}{\partial x}+v\frac{\partial w}{\partial y}+z\frac{\partial w}{\partial z}\right)=\rho g_z-\frac{\partial p}{\partial z}+\mu\left(\frac{\partial^2 w}{\partial x^2}+\frac{\partial^2 w}{\partial y^2}+\frac{\partial^2 w}{\partial z^2}\right) \tag{4}$$

Where:
u, v, w ⟶ flow velocities in the directions x, y and z respectively; ρ ⟶ fluid density; μ ⟶ dynamic viscosity of the fluid; g ⟶ gravity; p ⟶ pressure.

The difficulty of solving the equations analytically led to the development of Computational Fluid Dynamics as an alternative method of resolution since, according to Fortuna (2000), the mathematical theory of this class of equations is

not yet sufficiently developed to allow the obtainment of analytical solutions in arbitrary regions and general boundary conditions.

For the particular case of the Couette flow in a transient regime, a numerical model was developed to analyze its velocity profile under the hypothesis of an incompressible fluid in a one-dimensional flow, comparing it with the analytical solution of the problem in order to validate the model investigating its behavior according to different parameters and evaluating the best time intervals and spatial discretization that would provide greater accuracy at a lower computational cost to simulate this flow.

Therefore, a finite differences scheme was used and it consists of the approximation of Partial Differential Equations by their discretization in algebraic equations. In temporal discretization, the semi-implicit Crank-Nicolson scheme was adopted because it constitutes an unconditionally stable method, thus avoiding that the errors of numerical solution were amplified. However, since numerical methods use the approximations, it is necessary to establish stability criteria - Courant–Friedrichs–Lewy (CFL) condition - on the mathematical model in order to ensure reliable results by its approximation of the exact solution and, consequently, establishing adequate representation of the physical phenomena.

2. METHODOLOGY

2.1 Governing Equations

According to Munson et al (2004) and White (2011), the Couette Flow is characterized by the flow between two parallel plates in which one is fixed and the other has velocity U separated by a distance D.

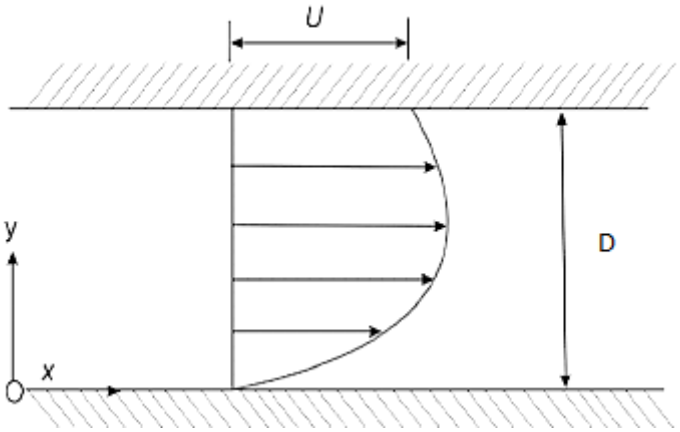

Figure 1. Couette flow between two plates. From: Mathur, Jajal and Singh (2017)

Consider the direction of flow on the x-axis and the distance between the plates belonging to the y-axis. Suppose the size of the plates on the z-axis is infinite, so that there is no variation of the flow in this direction. Thus, as presented in the works of Baheri and Navaserarab (2015) and Mathur, Jajal and Singh (2017) for the permanent regime, the ruling equation is:

$$\frac{\partial^2 u}{\partial y^2} = \frac{1}{\mu}\frac{\partial p}{\partial x} \tag{5}$$

Integrating Eq. (5) twice, it obtains:

$$u = \frac{y^2}{2\mu}\frac{\partial p}{\partial x} + c_1 y + c_2 \tag{6}$$

For the problem, the boundary conditions u(y=0) = 0 and for the fixed plate and u(y=D) = U for the plate with velocity U, the constants c1 and c2 are respectively:

$$c_1 = \frac{U}{D} - \frac{D}{2\mu}\frac{\partial p}{\partial x}, \qquad c_2 = 0 \tag{7}$$

The velocity profile equation takes the form:

$$u = \frac{U}{D}y - \frac{D^2}{2\mu}\frac{\partial p}{\partial x}\frac{y}{D}\left(1 - \frac{y}{D}\right) \tag{8}$$

and for non-dimensional analysis:

$$\frac{u}{U} = \frac{y}{D}\left(1 + P\left(1 - \frac{y}{D}\right)\right) \tag{9}$$

where

$$P = -\frac{D^2}{2\mu U}\frac{\partial p}{\partial x} \tag{10}$$

is a negative coefficient since the pressure gradient is opposite to the flow direction.

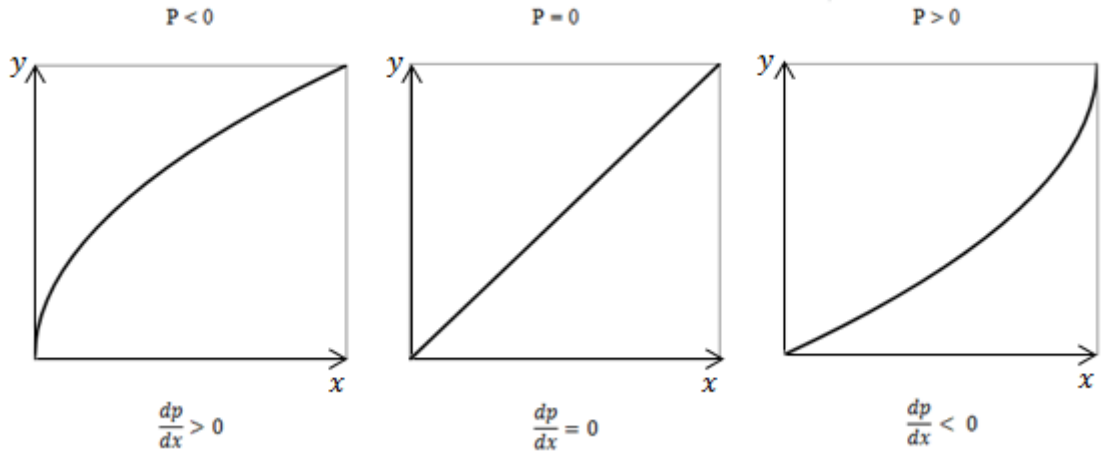

Figure 2. Velocity profiles with variation in pressure gradient. From: Author (2018)

For P > 0, i.e. when the pressure gradient $\frac{\partial p}{\partial x}$ is negative, it is favorable to the flow direction and velocity is positive throughout the interval between the two plates. For P < 0, $\frac{\partial p}{\partial x}$ is positive and opposite to movement and velocity may become negative with increasing pressure gradient.

The mathematical formulation suppose a transient flow in order to create the numerical model for this application in a finite differences under semi-implicit temporal discretization. The equation below describes the flow for the transient regime:

$$\rho\frac{\partial u}{\partial t} = \mu\frac{\partial^2 u}{\partial y^2} - \frac{\partial p}{\partial x} \tag{11}$$

The variables velocity (u), time (t) and distance between plates (y) are non-dimensioned as $u' = \frac{u}{U}, y' = \frac{y}{D}, t' = \frac{U}{D}t$:

$$\frac{\partial(u'U)}{\partial(Dt'/U)} = \frac{1}{Re}\frac{\partial^2(u'U)}{\partial(y'D)^2} + \frac{2P}{Re} \tag{12}$$

The equation, therefore, assumes the following form:

$$\frac{\partial u'}{\partial t'} = \frac{1}{Re}\frac{\partial^2 u'}{\partial y'^2} + \frac{2P}{Re} \tag{13}$$

where:

$Re = \frac{\rho DU}{\mu} \longrightarrow$ Reynolds number.

2.2 Numerical method

The Finite Differences method is applied by the Crank-Nicolson semi-implicit discretization because it constitutes an unconditionally stable numerical method with order error $O(\Delta t)^2$. According Fletcher (1988), the Eq. (13) can be written as:

$$\frac{u_i^{n+1} - u_i^n}{\Delta t} = \frac{1}{Re}\left(\frac{u_{i+1}^{n+1} - 2u_i^{n+1} + u_{i-1}^{n+1} + u_{i+1}^n - 2u_i^n + u_{i-1}^n}{2\Delta y^2}\right) + \frac{2P}{Re} \tag{14}$$

i.e.:

$$-su_{i-1}^{n+1} + (1+2s)u_i^{n+1} - su_{i+1}^{n+1} = k_i^n \tag{15}$$

where

$$k_i^n = su_{i+1}^n + (1-2s)u_i^n + su_{i-1}^n + \frac{2P}{Re}\Delta t \tag{16}$$

and

$$s = \frac{\Delta t}{2Re(\Delta y)^2} \tag{17}$$

For:
$i + 1 \longrightarrow$ subsequent spatial level;
$i \longrightarrow$ present spatial level;
$i - 1 \longrightarrow$ precedent spatial level;
$n + 1 \longrightarrow$ subsequent time level;
$n \longrightarrow$ present time level.

Despite the Crank-Nicolson Method is unconditionally stable, i.e., stable for all values of Δt, to ensure a real simulation in time and to minimize time-related truncation errors, it is relevant to establish a stability criterion, condition CFL:

$$\Delta t = E \times Re(\Delta y)^2 \tag{18}$$

where:

$E \longrightarrow$ a parameter of the condition.

This parameter can assume any value since the applied method ensures unconditional stability. It was adopted, then, E = 1.

The system of equations generated that has the same number of unknowns and equations which are linearly independent admits a unique solution and results in a tridiagonal square matrix that can be solved by the Thomas Algorithm, a particular case of Gaussian Elimination.

2.3 Programming language and machine used

The numerical solution was implemented computationally through code developed in Python language. The machine used for the simulation has the following technical specifications of the system: Manufacturer: ASUSTek Computer Inc.; Model: X556URK; Processor: Intel (R) Core (TM) i5-7200U CPU @ 2.50GHz 2.71 GHz; Installed memory (RAM): 8.00 GB (usable: 7.88 GB); System Type: 64-bit Operating System, x64-based processor; Hard Disk (HD): 1TB hard drive; Video Card: NVIDIA GeForce 2.00 GB.

3. RESULTS AND DISCUSSION

The analysis was realized for the cases: Re = 500/1000/2000; P = -1/0/1. The numerical solutions were obtained for the parameters indicated below: N = 25/100/500 - number of spatial intervals; t = 100 s / 500 s.

The error between the numerical solution as a function of the spatial discretization and the analytical solution is calculated for each Reynolds number and non-dimensional coefficient whose signal indicates the variation of the pressure gradient in the percentage of the number of time steps obtained by the discretization of the interval of 500 s.

The velocity profiles for the Reynolds number Re = 2000 and the non-dimensional coefficients equivalent to P = -1 and P = 1 are shown in Fig. 3 and 4.

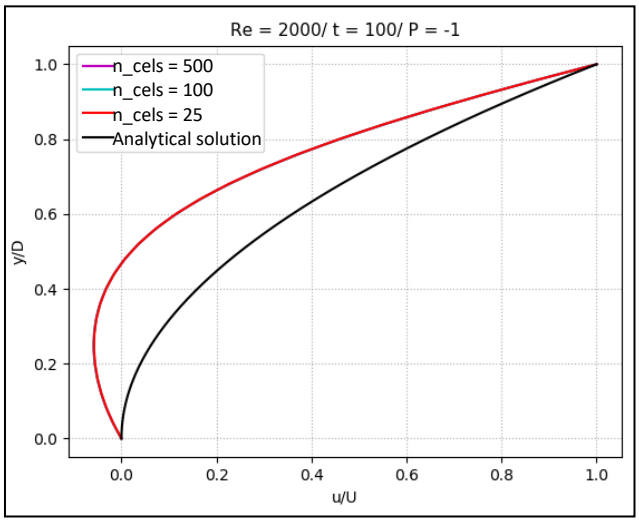

Figure 3. Velocity Profile. From: Author (2018)

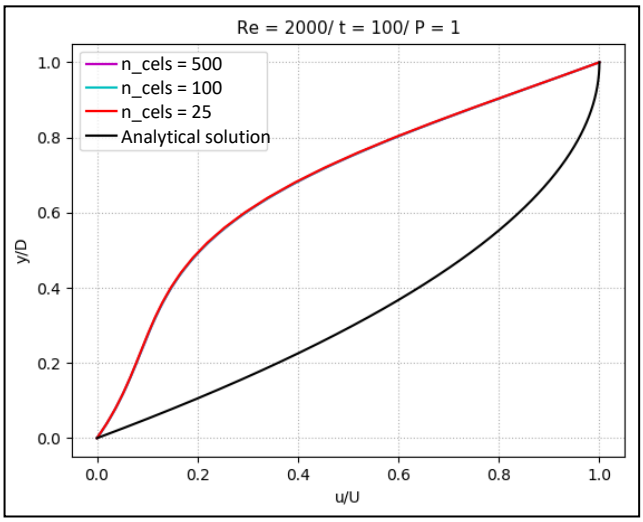

Figure 4. Velocity Profile. From: Author (2018)

Figures 5 and 6 present the velocity profiles for Reynolds number Re = 2000 and null pressure. It is possible to observe their differences in relation to the evolution in time: from t = 100 s (Fig. 5) to t = 500 s (Fig. 6).

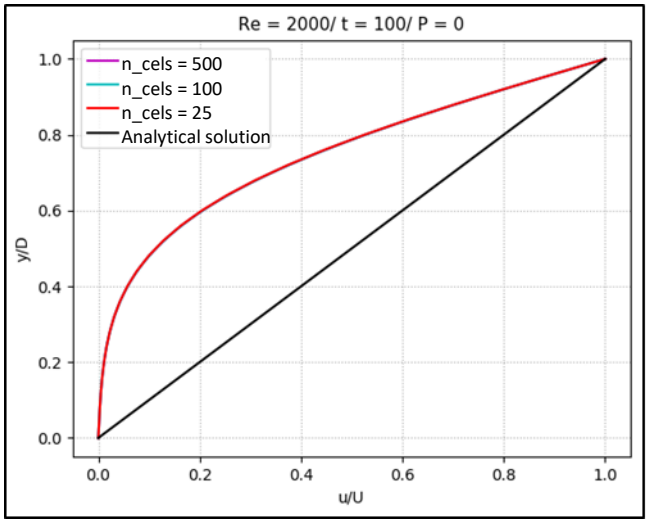

Figure 5. Velocity Profile. From: Author (2018)

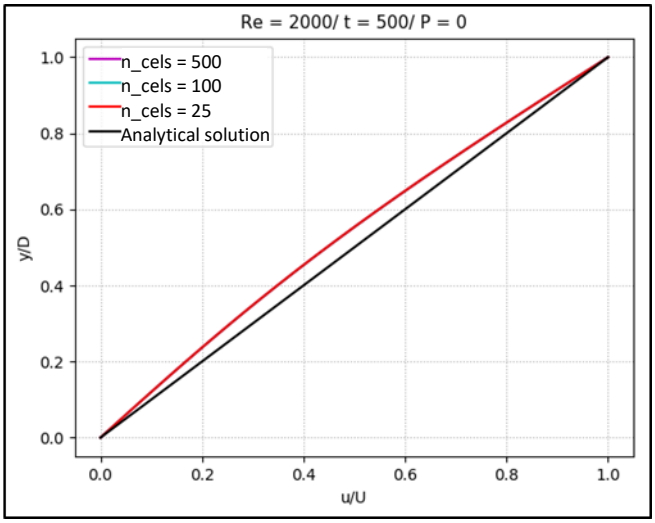

Figure 6. Velocity Profile. From: Author (2018)

Figure 7 shows the difference between the numerical and analytical solutions by calculating the maximum error with the evolution of time (i / step). That reason can be translated as the percentage of the number of time steps where i represents the variation of the number of steps in relation to their total interval (step). Table 1 shows the maximum error for the time equal to 500 s according to graphic of Figure 7 in order to visualize the differences between error quantities for each number of cells.

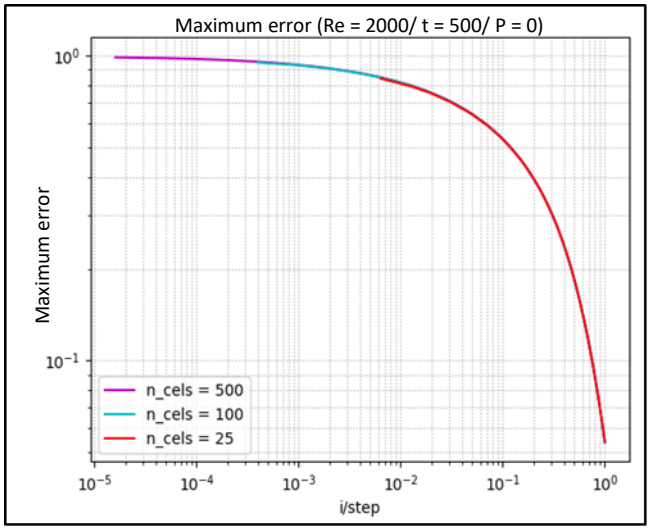

Figure 7. Maximum error versus percentage of time steps. From: Author (2018)

Table 1. Maximum error in relation to number of cells for the time equal to 500 s. From: Author (2019)

n_cels	Maximum error (t = 500s)
500	0.05398
100	0.05399
25	0.54198

For the numerical solution to reach the steady-state, is was simulated for a relatively large time interval (t = 1000s), according to Figure 8 and with the accuracy presented in Table 2. It was adopted the error of 5.10^{-3} as satisfactory accuracy to the numerical solution to reach the steady-state. For n_cels = 500, the accuracy was greater but other values also reached the satisfactory accuracy. The same precision was considered for the simulation of other cases as shown in Table 3, 4 and 5.

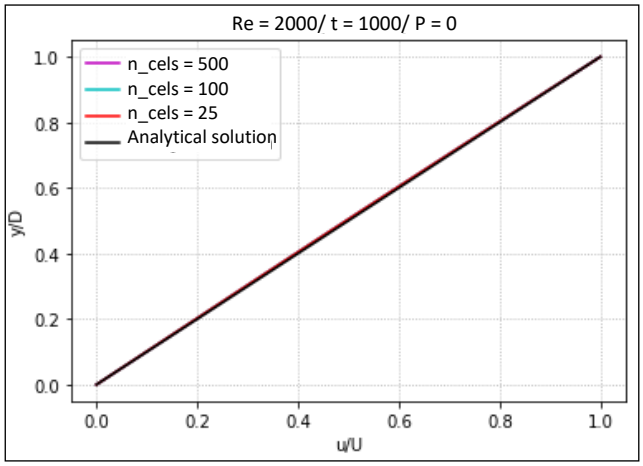

Figure 8. Velocity Profile. From: Author (2019)

Table 2. Maximum error in relation to number of cells for the indicated time. From: Author (2019)

n_cels	Maximum error (t = 1000s)
500	0.00458
100	0.00458
25	0.00463

Figures 5, 9 and 10 show the results of the velocity profiles for P = 0 with variation in the Reynolds number.

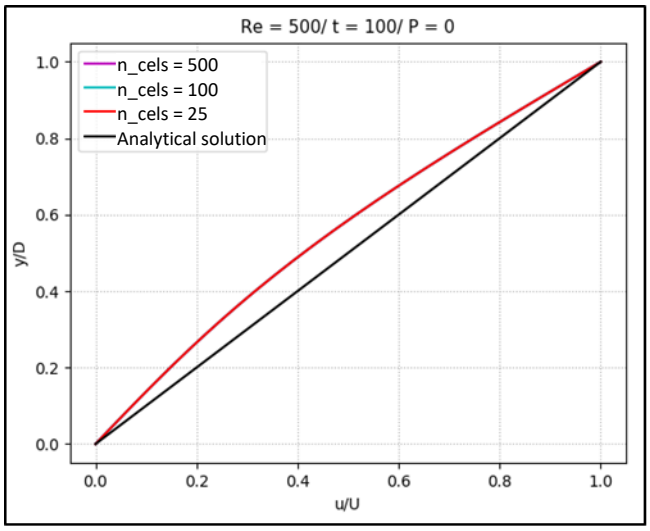

Figure 9. Speed Profile. From: Author (2018)

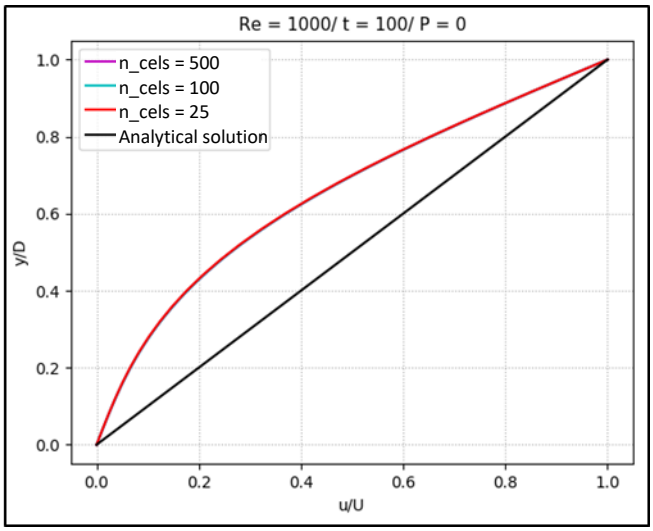

Figure 10. Speed Profile. From: Author (2018)

The tables below show the runtime and the accuracy of the simulations for each configuration.

Table 3. Runtime for P = -1. From: Author (2019)

P = -1				
Re	t (s)	n_cels	Maximum error	Runtime of tool (s)
500	100	500	0.052593	189.11
		100	0.052594	1.52
		25	0.052522	0.03
	500	500	0.000020	971.86
		100	0.000020	7.64
		25	0.000020	0.12
Re	t (s)	n_cels	Maximum error	Runtime of tool (s)
1000	100	500	0.14161	94.02
		100	0.14160	0.77
		25	0.14259	0.02
	500	500	0.00272	473.48
		100	0.00272	3.80
		25	0.00275	0.06

Re	t (s)	n_cels	Maximum error	Runtime of tool (s)
2000	100	500	0.24441	48.43
		100	0.24437	0.41
		25	0.24530	0.00
	500	500	0.03211	241.71
		100	0.03211	2.16
		25	0.03220	0.03
	1000	500	0.00272	484.38
		100	0.00272	4.00
		25	0.00275	0.06

Table 4. Runtime for P = 0. From: Author (2019)

P = 0				
Re	t (s)	n_cels	Maximum error	Runtime of tool (s)
500	100	500	0.08843	159.99
		100	0.08844	1.19
		25	0.08838	0.02
	500	500	0.00003	841.22
		100	0.00003	5.80
		25	0.00003	0.09
Re	t (s)	n_cels	Maximum error	Runtime of tool (s)
1000	100	500	0.23756	73.65
		100	0.23755	0.57
		25	0.23944	0.01
	500	500	0.00458	394.62
		100	0.00458	2.91
		25	0.00463	0.05
Re	t (s)	n_cels	Maximum error	Runtime of tool (s)
2000	100	500	0.39610	37.44
		100	0.39609	0.29
		25	0.39732	0.01
	500	500	0.05398	184.24
		100	0.05399	1.44
		25	0.54198	0.05
	1000	500	0.00458	384.00
		100	0.00458	3.18
		25	0.00463	0.05

Table 5. Runtime for P = 1. From: Author (2019)

P = 1				
Re	t (s)	n_cels	Maximum error	Runtime of tool (s)
500	100	500	0.12428	158.98
		100	0.12429	1.19
		25	0.12425	0.02
	500	500	0.00005	847.14
		100	0.00005	8.06
		25	0.00005	0.16
Re	t (s)	n_cels	Maximum error	Runtime of tool (s)
1000	100	500	0.33363	74.60
		100	0.33364	0.59
		25	0.33630	0.02
	500	500	0.00643	484.88
		100	0.00644	4.05
		25	0.00651	0.06
	600	500	0.00240	582.34
		100	0.00240	4.55
		25	0.00241	0.08
Re	t (s)	n_cels	Maximum error	Runtime of tool (s)
2000	100	500	0.55075	48.65
		100	0.55074	0.39
		25	0.55265	0.02
	500	500	0.07587	242.21
		100	0.07588	1.94
		25	0.07619	0.03
	1000	500	0.00643	483.92
		100	0.00644	3.97
		25	0.00651	0.06
	1100	500	0.00393	533.74
		100	0.00393	4.19
		25	0.00399	0.09

4. CONCLUSION

Figures 5, 9 and 10 present the variation of the velocity profile according to the Reynolds number and, with the increase of Δt due to that parameter to be dependent of Re as presented by Eq. (18), the difference between the numerical and analytical solutions is greater. The explanation is that the calculation of Δt is a function of the Reynolds number. In this way, the discretization is less refined since Δt is larger.

Analyzing Figs. 5, 6 and 8, it concludes that, with the advancement of time, i.e., the increase in the number of iterations, the numerical solution approaches the analytical solution since the simulation was achieved until to be reached the steady-state. From the Tables 1 and 2, it is observed the level of accuracy of the simulations as a function of time and

number of cells presenting better result when the number of cells is greater. From these tables, it can conclude that, for a more refined spatial discretization, i.e., for a larger number of cells, the resulting error will be smaller. Number of cells n_cels = 500 presented lower error.

The graphic of Fig. 7 shows the decay of the error as a function of the percentage of time steps which confirms the greater proximity between the solutions with the evolution of time until reached the steady-state as shown in Table 2.

The Finite Differences Method, therefore, it was satisfactory in the analysis of the velocity profile under evaluation of varied parameters, obtaining better results in relation to accuracy for longer spatial discretization (n_cels = 500 according to the configurations used in this work). However in relation to runtime of tool, for small spatial discretization, the tool obtained a shorter runtime with satisfactory accuracy according to time interval required to reach the steady-state as shown in Tables 3, 4 and 5.

5. REFERENCES

BAHERI, A; NAVASERARAB, A. “Impact of the Time Interval in the Numerical Solution of Incompressible Flows”. International Journal of Scientific Engineering and Applied Science (IJSEAS), Dezful - Iran. v. 1. Issue-4, 2015.

FLETCHER, C. A. “Computational Techniques for Fluid Dynamics”, vol. II: Specific Techniques for Different Flow Categories, Springer-Verlag, Berlin, 1988.

FORTUNA, A. O. “Técnicas Computacionais para Dinâmica dos Fluidos”. EDUSP, São Paulo- SP, p.19-211. 2000.

MATHUR, M; JAJAL, N.A; SINGH, R. K. “Finite difference solver for couette flow with applied pressure gradients”. International Journal of Advance Research and Innovation, Delhi 42- India. v. 5 Issue-2, 2017.

MUNSON, B.R.; YOUNG, D.F.; OKIISHI, T. H. “Fundamentos da Mecânica dos Fluidos”. Editora Edgard Blücher, 1 ed. São Paulo- SP, p. 311-.317. 2004.

THAPA, D. B; UPRETY, K. N. “Analytic and Numerical Solutions of Couette Flow Problem: A Comparative Study”. Journal of the Institute of Engineering, TUTA/IOE/PCU – Nepal.12(1): 105-113,2016.

WHITE, F. M. “Mecânica dos Fluidos”. AMGH Editora Ltda, 6. ed. – Porto Alegre - RS, p.276-284. 2011.

6. RESPONSIBILITY NOTICE

The authors are solely responsible for the printed material contained in this article.